# Potentials for $\alpha$+$^{116,122,124}$Sn elastic scattering

Shuva Saha, Faria Ahmed, Dipika Rani Sarker and M. Nure Alam Abdullah

Department of Physics, Jagannath University, Dhaka-1100 Bangladesh

LXXI International Conference "NUCLEUS-2021. Nuclear physics and elementary particle physics. Nuclear physics technologies"

# Introduction

- Nuclear structure → nucleus-nucleus interaction potential
- Nuclear scattering due to nuclear forces (to analyse the experimental angular distribution of the emitted particles)

↓

Nuclear potential

- The optical model (OM) potential is pretty well known to explain the phenomena.
- Alpha-particle elastic scattering → ALAS (Anomaly in Large Angle Scattering)
- ALAS is prominent but not unique to A ≈ 4n (n = 1, 2, 3, …) nuclei and for A ≤ 50.
- Beyond this region, the ALAS effect rapidly dies down giving rise to the "rainbow scattering".

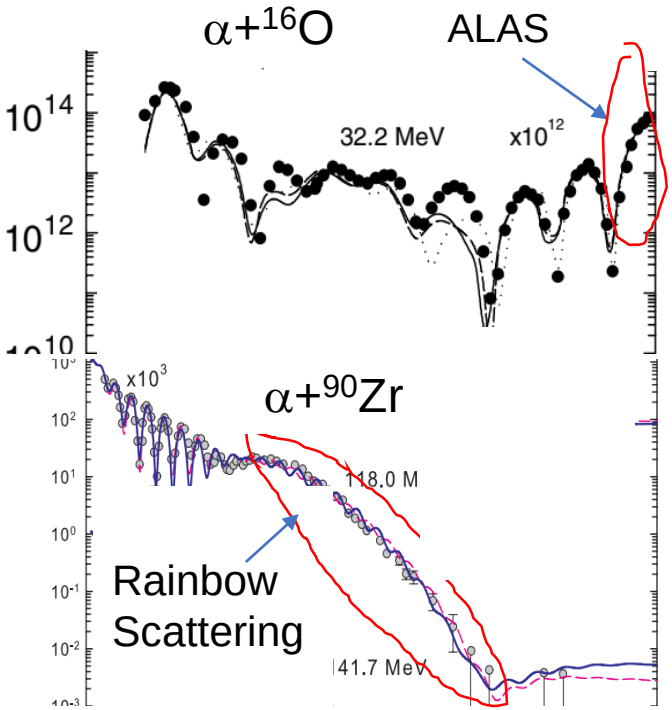


*K.W. Kemper, A.W. Obst and and R.L. White, Phys. Rev. C 6 (1972) 2090.*
*L. Jarczyk et al., Acta Phys. Pol. B 7 (1976) 53.*

# Introduction

## Optical model (OM) potential

Phenomenological OM potential
(obtained empirically from the direct analysis of the elastic scattering data)

(i) Woods-Saxon (WS)
(ii) squared Woods-Saxon (SWS)

suffer from discrete ambiguity

OM potentials is derived microscopically or semi-microscopically

(i) Folded (double folded, single-folded)
(ii) non-monotonic (NM) - derived from the EDF theory of Brueckner, Coon and Dabrowski (BCD).

*K.W. Kemper, A.W. Obst and R.L. White, Phys. Rev. C 6 (1972) 2090.*
*F. Michel et al, Phys. Rev. C 28 (1983) 1904.*

*M. E. Brandan and G. R. Satchler Phys. Rep. 285 (1997) 143.*
*M. N. A. Abdullah et al, Eur Phys J. A 18 (2003) 65*
*M. N. A. Abdullah et al, Nucl. Phys. A 760 (2005) 40.*
*K. A. Brueckner, S. A. Coon and J. Dabrowski, Phys. Rev. 168 (1968) 1184.*

# Introduction

- Traditional double folded (DF) of effective *N-N* interaction and single folded (SF) of either $\alpha$-*N* or $\alpha$–$\alpha$ potentials need renormalizations at different incident energies.

- In 2003, we proposed a single-folding model the resulting potential from which does not need any renormalization.

- *M. N. A. Abdullah et al., Eur. Phys. J. A 18 (2003) 65.*
- *M. N. A. Abdullah et al., Phys. Lett. B 571 (2003) 45.*

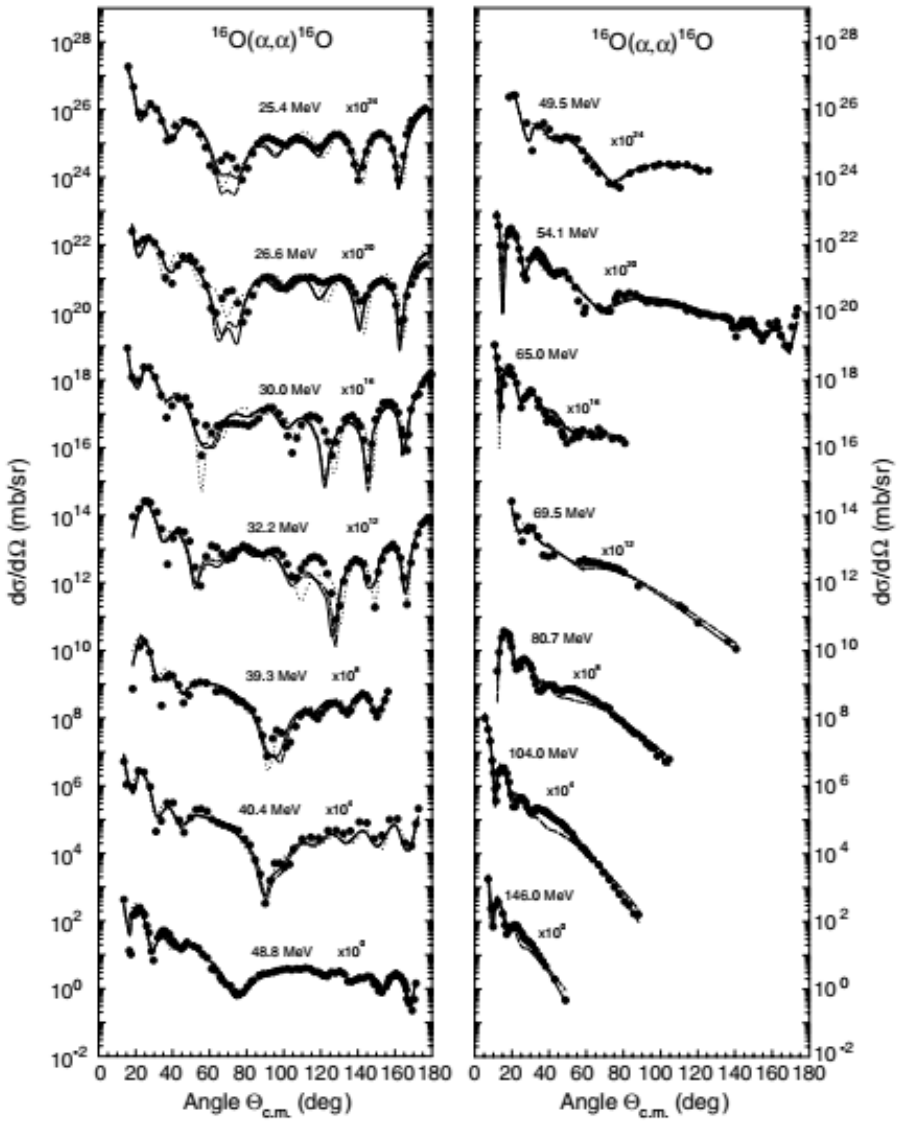


*M. N. A. Abdullah et al., Eur. Phys. J. A 18 (2003) 65*

# Our Folding Model

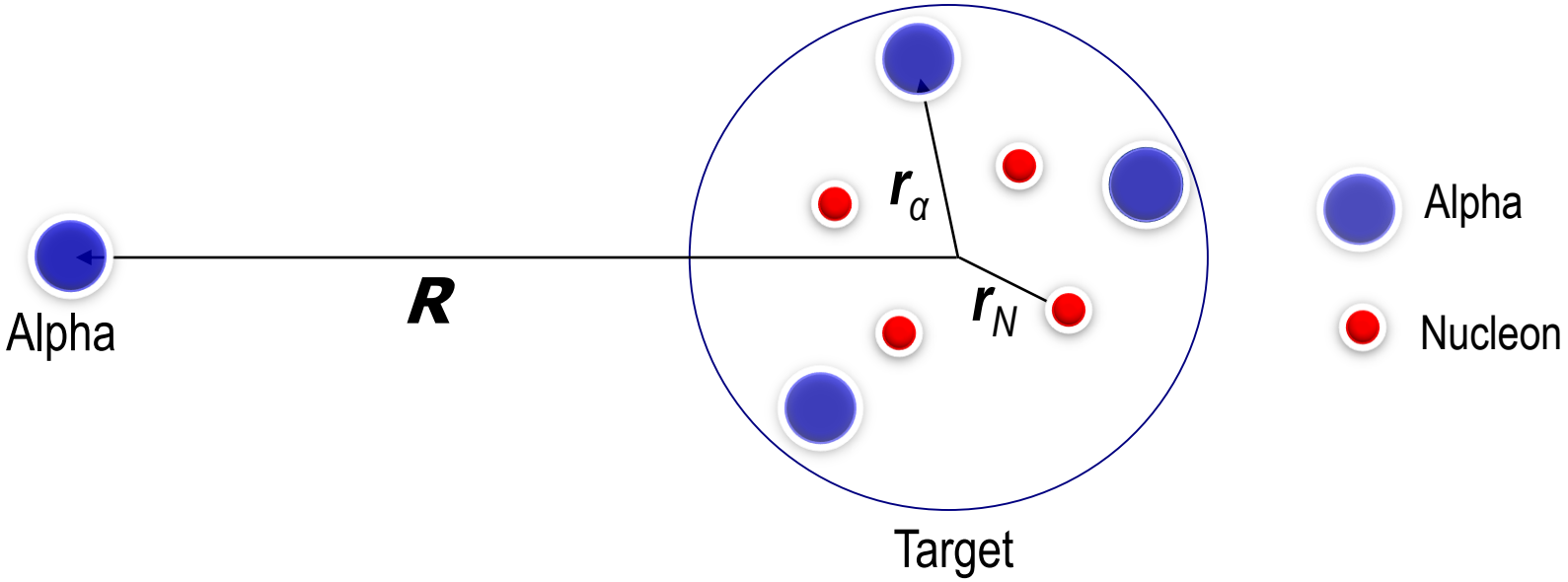


Assumptions:

i. the nucleons in the target are considered primarily in the $\alpha$–cluster configuration, and rest in an unclustered nucleonic configuration

ii. the wave function of a nucleus can be considered as the product of wave functions of $\alpha$-like configurations and those of unclustered nucleonic configurations

iii. This leads to a sum of two folding potentials, one convoluted over $\alpha$-density distribution and another over nucleonic density distribution.

# MSF Potential

The modified single folded (MSF) real nuclear potential:

$$U(R) = \int \rho_\alpha(\vec{r}_\alpha) V_{\alpha\alpha}\left(\left|\vec{R} - \vec{r}_\alpha\right|\right) d^3\vec{r}_\alpha + \int \rho_N(\vec{r}_N) V_{\alpha N}\left(\left|\vec{R} - \vec{r}_N\right|\right) d^3\vec{r}_N. \quad (1)$$

α–α potential: $V_{\alpha\alpha}(r) = V_R\, exp(-{\mu_R}^2 r^2) - V_A\, exp(-{\mu_A}^2 r^2).$ (2)

α–N potential: $V_{\alpha N}(r) = -V_0\, exp(-k^2 r^2).$ (3)

The parameter values are:

$V_A$ = 122.62 MeV, $\mu_A$ = 0.469 fm$^{-1}$

[*B. Buck, H. Friedrich, C. Wheatley, Nucl. Phys. A 275 (1977) 241.*]

$V_0$ = 47.3 MeV and $K$ = 0.435 fm$^{-1}$

[*S. Sack, L. C. Biedenharn, G. Breit, Phys. Rev. 93 (1954) 321.*]

Density distribution (2pF) used:

$$\rho_i(r) = \rho_{0i}\left[1 + exp\left(\frac{r - c_i}{a_i}\right)\right]^{-1}, \text{ with } i = \alpha, N \quad (4)$$

# MSF Potential

The Imaginary potential: $$W(R) = -W_0 \, exp\left(-\frac{R^2}{{R_W}^2}\right). \quad (5)$$

Coulomb potential: $$V_C(R) = \begin{cases} \frac{Z_1 Z_2 e^2}{2R_C}\left(3 - \frac{R^2}{{R_C}^2}\right), & R \le R_C \\ \frac{Z_1 Z_2 e^2}{2r}, & R > R_C. \end{cases} \quad (6)$$

with $R_C = 1.35 \times A^{1/3}$.

Normalization integral: $$\int \rho_\alpha(\vec{r}_\alpha) d^3\vec{r}_\alpha + \int \rho_N(\vec{r}_N) d^3\vec{r}_N = 4A_\alpha + A_N = A_T \, . \quad (7)$$

# Non-monotonic (NM) potential

The analytic form of the NM potential:

Real part:

$$V_{NM}(r) = -V_0\left[1 + exp\left(\frac{r - R_0}{a_0}\right)\right]^{-1} + V_1 exp\left[-\left(\frac{r-D_1}{R_1}\right)^2\right] + V_C(r) \qquad (9)$$

The potential becomes non-monotonic with the inclusion of the second term.

Imaginary part:

$$W_{NM}(r) = -W_0 exp\left[-\left(\frac{r}{R_W}\right)^2\right] - W_S exp\left[-\left(\frac{r-D_S}{R_S}\right)^2\right]. \qquad (10)$$

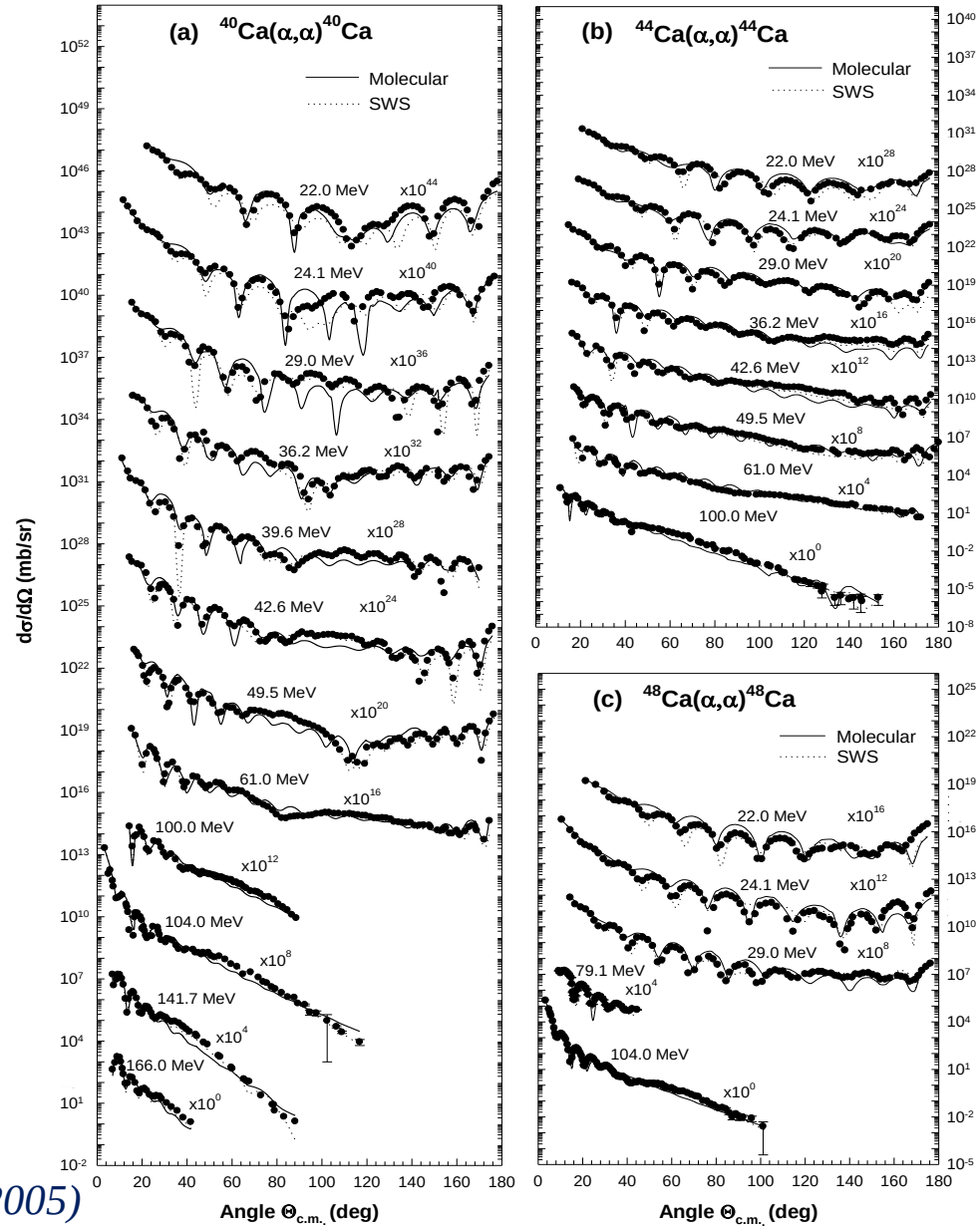


[*M. N. A. Abdullah et al, Nucl. Phys. A 760 (2005) 40.*]

# Non-monotonic (NM) potential

- Hossain *et al*. explained the refractive structure of $\alpha$+$^{90}$Zr elastic scattering using the NM potential derived from the EDF theory.

- The potential in the central region of the target nucleus seems to be significant in describing the $\alpha$ elastic scattering data on $^{90}$Zr.

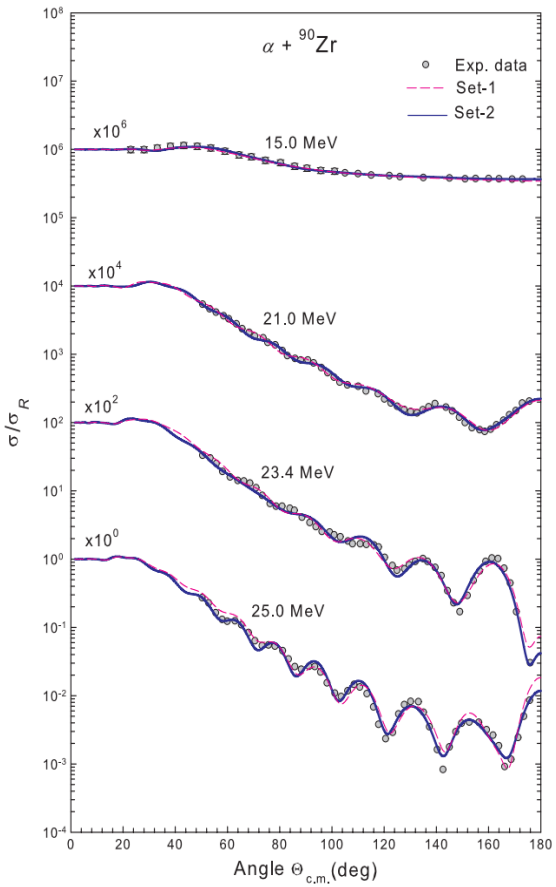


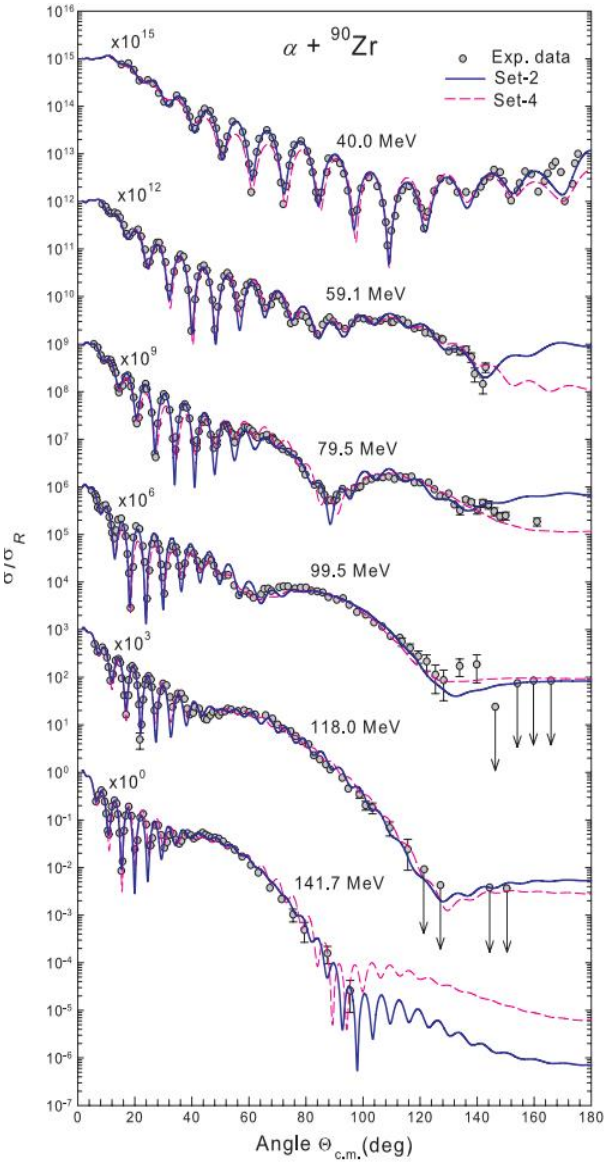


*S. Hossain et al, J. Phys. G: Nucl. Part. Phys. 40 (2013) 105109.*

# Non-monotonic (NM) potential

Basak *et al.* successfully extended the approach of using the NM potential, derived from a realistic two-nucleon (NN) potential using the EDF method, to reproduce simultaneously

- the elastic scattering cross-sections and
- the vector analyzing power data for $^{6,7}$Li projectiles on $^{12}$C, $^{26}$Mg, $^{58}$Ni and $^{120}$Sn
- without adjusting the shape or depth parameters of the EDF-derived potentials.

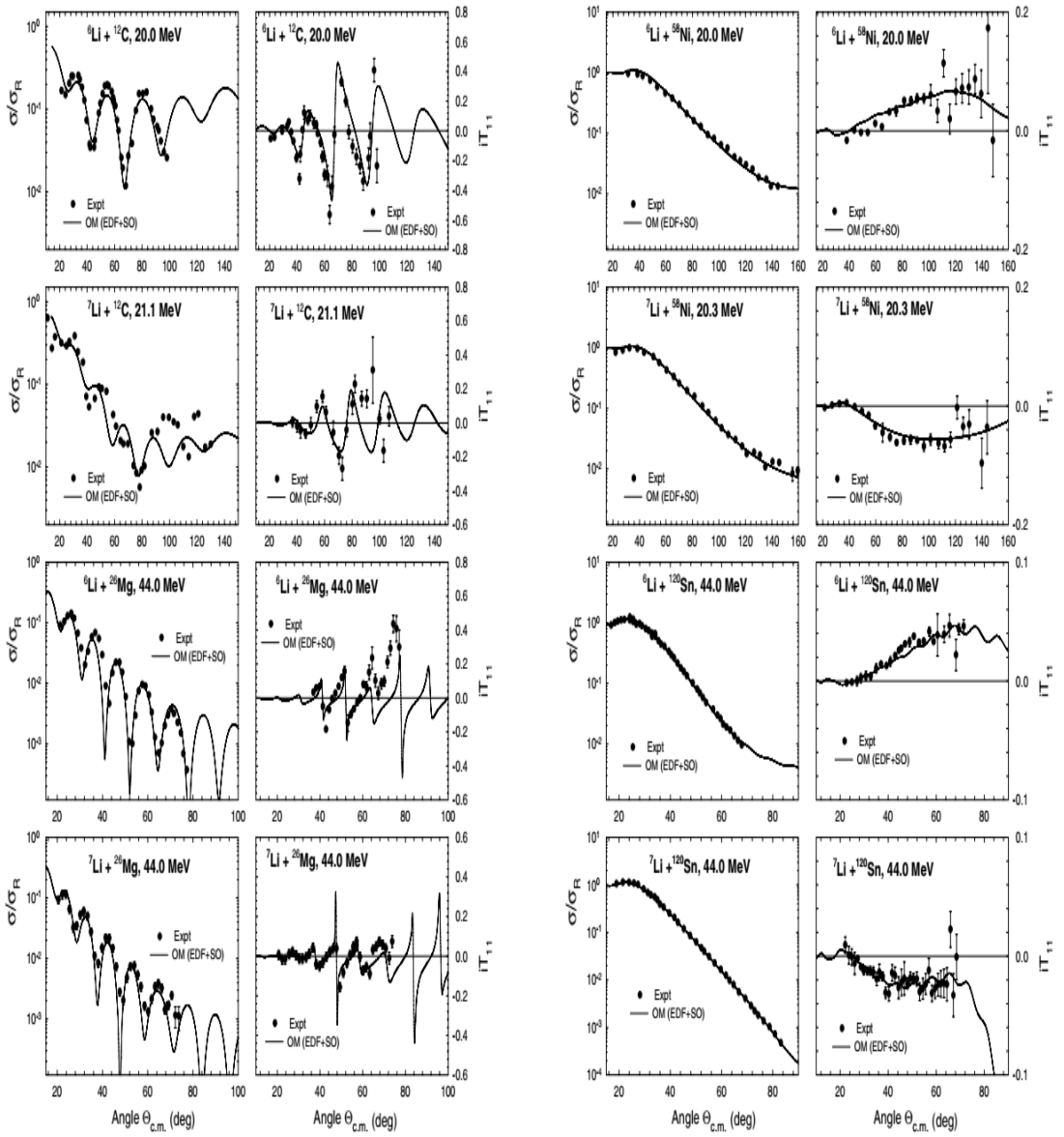


*A. K. Basak et al, Europhys. Lett. 94 (2011) 62002.*

# Non-monotonic (NM) potential

Strikingly, their analysis correctly described the observed opposite signs in the elastic scattering VAP data for $^{6}$Li and $^{7}$Li of the same energy incident on $^{58}$Ni and $^{120}$Sn nuclei.

These successes are attributed to the following features:

(i) the NM nature of the central real potential arising from the use of the Pauli effect in the EDF theory

(ii) optimum use of empirical absorption

(iii) an appropriate choice of the effective SO potential of either sign, being a manifestation of the projectile excitation process.

# Analysis

Code used:

SCAT2 *[O. Bersillon, The code SCAT2, NEA 0829, private communication.*

SFRESCO which incorporates the coupled-channels code FRESCO 2.5
[*I. J. Thompson. Comp. Phys. Rep. 7 (1988) 167.]*

MINUIT [*F. James and M. Roos, Comp. Phys. Commun. 10 (1975) 343.]*

A set of parameters is obtained by minimizing $\chi^2$ defined as:

$$\chi^2 = \frac{1}{N}\sum_i \left[\frac{\sigma_{exp}(\Theta_i) - \sigma_{th}(\Theta_i)}{\Delta\sigma_{exp}(\Theta_i)}\right]^2. \qquad (8)$$

# Results of MSF

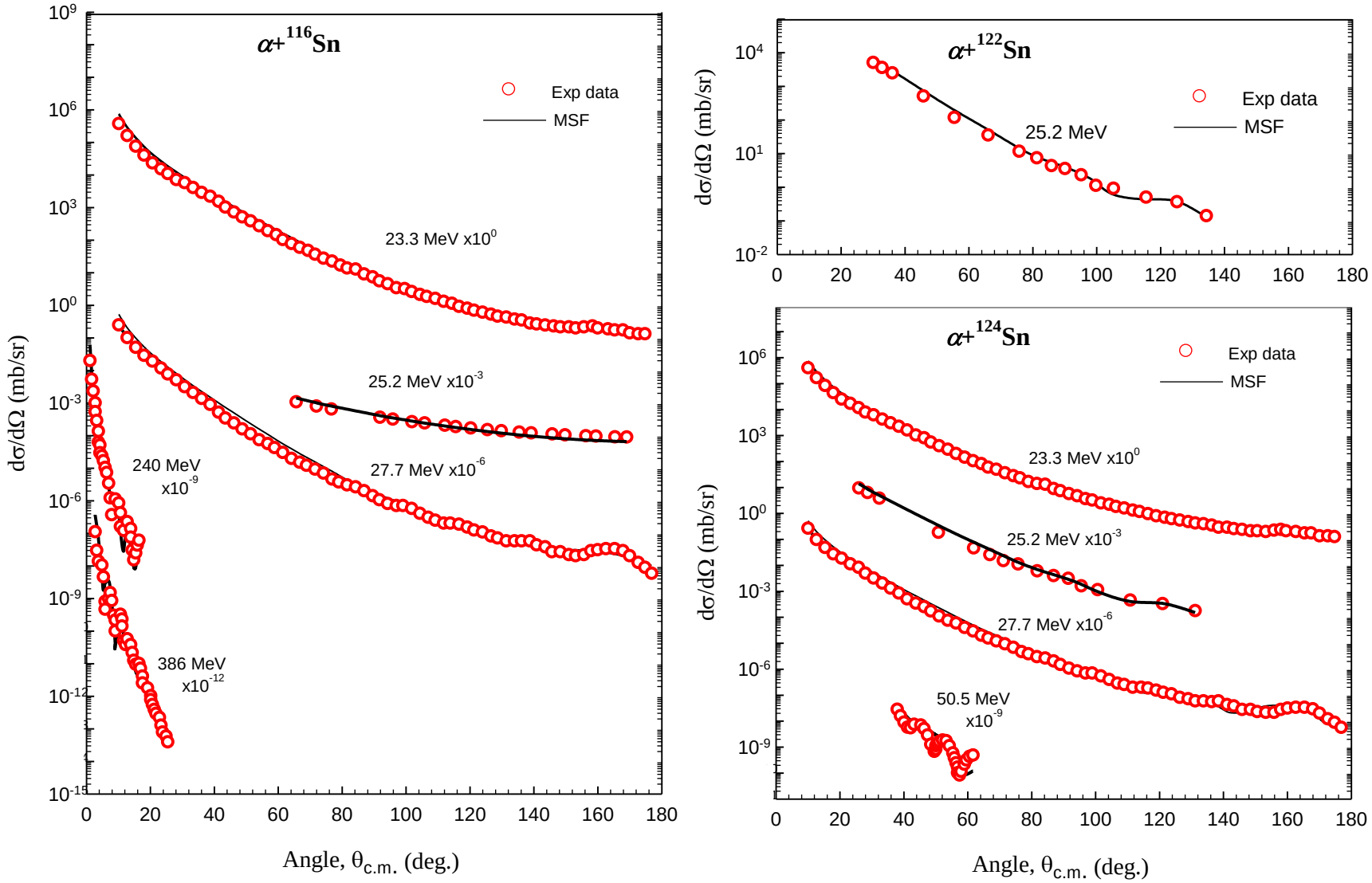


**Fig. 2**. The predicted cross sections for the $\alpha$+$^{116,122,124}$Sn elastic scattering using the MSF potentials at different incident energies. The open circles are the experimental data.

# Results of MSF

**Table 1.** Energy independent parameters and the deduced results for $\alpha$+$^{208}$Pb elastic scattering. $\rho_{0\alpha}$ and $\rho_{0N}$ are in fm$^{-3}$; $c_\alpha$, $c_N$, $a_\alpha = a_N$ and $R_{rms}$ in fm.

| Target | $\rho_{0\alpha}$ | $\rho_{0N}$ | $c_\alpha$ | $c_N$ | $a_\alpha = a_N$ | $4A_\alpha$ | $A_N$ | $A_T$ |
|---|---|---|---|---|---|---|---|---|
| $^{116}$Sn | 0.03093 | 0.1518 | 5.358 | 3.25 | 0.550 | 88.0 | 28.0 | 116 |
| $^{122}$Sn | 0.02948 | 0.1800 | 5.450 | 3.28 | 0.550 | 88.0 | 34.0 | 122 |
| $^{124}$Sn | 0.02903 | 0.1900 | 5.490 | 3.30 | 0.534 | 88.0 | 36.0 | 124 |

# Results of MSF

**Table 2.** Energy dependent parameters along-with the volume integrals and $\chi^2$. $E_a$, and the depth parameters $V_R$ and $W_0$ are in MeV; $\mu_R$ in fm$^{-1}$; $R_W$ in fm; and $J_R/(4A)$ and $J_I/(4A)$ in MeV.fm$^3$.

| Target | $E_\alpha$ | $V_R$ | $\mu_R$ | $W_0$ | $R_W$ | $J_R/(4A)$ | $J_I/(4A)$ | $\chi^2$ |
|---|---|---|---|---|---|---|---|---|
| $^{116}$Sn | 23.3 | 30.0 | 0.48 | 9.0 | 8.40 | -369.2 | -59.11 | 5.91 |
| | 25.2 | 31.0 | | 10.0 | 8.20 | -368.6 | -61.10 | 4.15 |
| | 27.7 | 41.0 | | 16.0 | 7.40 | -353.5 | -71.85 | 15.5 |
| | 240.0 | 160.0 | 0.58 | 32.0 | 7.05 | -251.6 | -124.3 | 18.8 |
| | 386.0 | 344.0 | | 220.0 | 3.75 | -162.5 | -128.6 | 128.6 |
| $^{122}$Sn | 25.2 | 32.5 | 0.48 | 10.0 | 8.00 | -382.2 | -53.95 | 4.11 |
| $^{124}$Sn | 23.3 | 39.0 | 0.48 | 10.0 | 8.00 | -374.1 | -53.08 | 4.95 |
| | 25.2 | 41.1 | | 11.0 | | -370.0 | -58.40 | 6.79 |
| | 27.7 | 49.0 | | 14.5 | 7.35 | -359.3 | -59.70 | 14.1 |
| | 50.5 | 50.0 | | 17.0 | | -357.4 | -70.00 | 54.1 |

# Results of NM

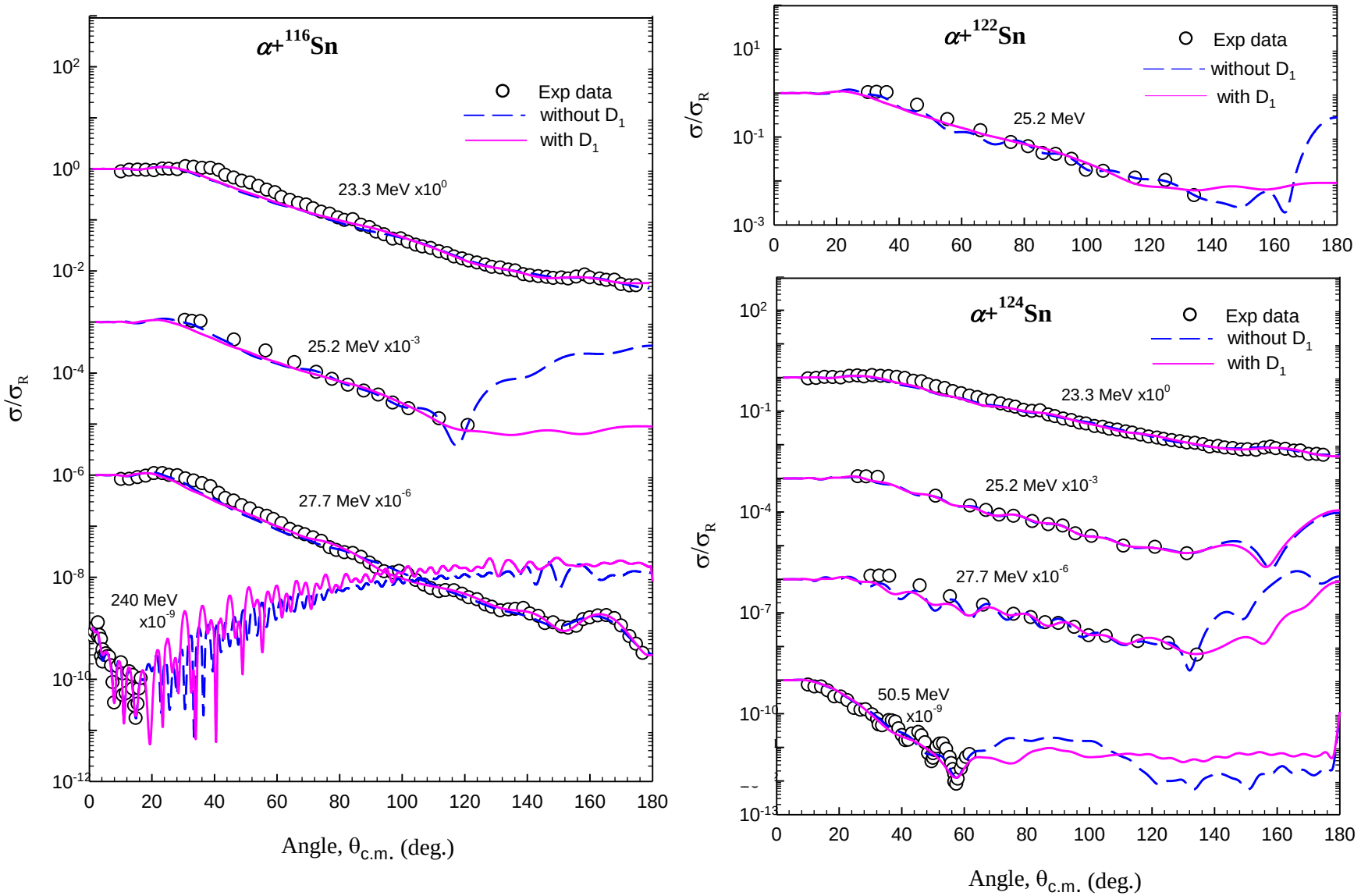


**Fig. 3**. The predicted cross sections for the $\alpha$+$^{116,122,124}$Sn elastic scattering at different incident energies using the NM potentials with unshifted repulsive core (blue broken lines) and shifted repulsive core (pink solid lines) are compared to the experimental data (open circles).

# Results of NM

Table 3. The real part of the NM potentials for the fits to the $\alpha$+$^{208}$Pb elastic scattering at different incident energies. $V_0$ and $V_1$ in MeV, and $R_0$, $a_0$, $D_1$, $R_1$ and $R_C$ in fm.

| Target | $E_\alpha$ | Set | $V_0$ | $R_0$ | $a_0$ | $V_1$ | $D_1$ | $R_1$ | $R_C$ | $J_R/(4A)$ |
|---|---|---|---|---|---|---|---|---|---|---|
| $^{116}$Sn | 23.3 | Set-1 | 26.5 | 6.466 | 0.30 | 250.0 | 0.00 | 0.6759 | 10.5 | -65.07 |
| | | Set-2 | 34.6 | 5.725 | 0.30 | 70.60 | 1.2678 | 0.8672 | | -54.33 |
| | 25.2 | Set-1 | 31.9 | 5.448 | 0.30 | 103.3 | 0.00 | 1.769 | | -41.09 |
| | | Set-2 | 34.4 | 5.725 | 0.30 | 70.60 | 1.2678 | 0.8672 | | -54.02 |
| | 27.2 | Set-1 | 32.6 | 5.504 | 0.30 | 10.20 | 0.00 | 0.4093 | | -50.58 |
| | | Set-2 | 34.5 | 5.575 | 0.30 | 110.5 | 1.1737 | 0.6362 | | -50.17 |
| | 240 | Set-1 | 34.0 | 4.970 | 0.30 | 26.80 | 0.00 | 1.8502 | | -37.02 |
| | | Set-2 | 26.7 | 5.422 | 0.30 | 121.0 | 1.3477 | 0.7771 | | -29.96 |
| 122Sn | 25.2 | Set-1 | 38.6 | 5.944 | 0.10 | 92.0 | 0.00 | 0.5700 | | -69.91 |
| | | Set-2 | 38.7 | 5.927 | 0.10 | 53.8 | 0.4959 | 0.2001 | | -69.41 |
| 124Sn | 23.3 | Set-1 | 34.1 | 6.637 | 0.204 | 40.0 | 0.00 | 0.2001 | | -84.89 |
| | | Set-2 | 37.0 | 6.344 | 0.173 | 100.0 | 0.6863 | 0.3150 | | -81.00 |
| | 25.2 | Set-1 | 29.0 | 6.662 | 0.15 | 76.2 | 0.00 | 0.2565 | | -72.86 |
| | | Set-2 | 32.3 | 6.447 | 0.103 | 30.0 | 0.5223 | 0.200 | | -73.41 |
| | 27.7 | Set-1 | 29.5 | 7.030 | 0.10 | 95.9 | 0.00 | 0.342 | | -86.8 |
| | | Set-2 | 35.2 | 6.577 | 0.10 | 41.9 | 0.7126 | 0.3576 | | -85.12 |
| | 50.5 | Set-1 | 33.8 | 7.002 | 0.512 | 74.9 | 0.00 | 0.5628 | | -71.6 |
| | | Set-2 | 40.0 | 7.003 | 0.113 | 99.8 | 1.1012 | 0.803 | | -71.3 |

# Results of NM

Table 4. The imaginary parameters of the NM potentials for fits to the $\alpha$+$^{208}$Pb elastic scattering data. $W_0$ and $Ws$ are in MeV; $R_S$, $R_W$, $D_S$ in fm; $J_I/(4A)$ in MeV.fm$^3$.

| Target | $E_\alpha$ | Set | $W_0$ | $R_W$ | $W_S$ | $D_S$ | $R_S$ | $J_I/(4A)$ | $\chi^2$ |
|---|---|---|---|---|---|---|---|---|---|
| $^{116}$Sn | 23.3 | Set-1 | 30.4 | 3.344 | 10.4 | 6.701 | 1.722 | -53.53 | 1.71 |
| | | Set-2 | 49.4 | 1.343 | 10.8 | 6.767 | 1.528 | -38.64 | 1.42 |
| | 25.2 | Set-1 | 102.0 | 1.247 | 8.0 | 7.136 | 0.406 | -41.09 | 1.03 |
| | | Set-2 | 55.0 | 1.344 | 10.8 | 6.766 | 1.528 | -38.80 | 2.25 |
| | 27.2 | Set-1 | 0.2 | 1.368 | 10.3 | 6.158 | 1.761 | -34.31 | 1.62 |
| | | Set-2 | 12.5 | 1.343 | 10.7 | 6.689 | 1.766 | -42.38 | 1.30 |
| | 240 | Set-1 | 41.5 | 1.652 | 9.9 | 6.433 | 2.00 | -43.08 | 2.39 |
| | | Set-2 | 52.0 | 1.607 | 11.4 | 6.183 | 1.923 | -44.92 | 2.39 |
| 122Sn | 25.2 | Set-1 | 3.8 | 1.253 | 4.5 | 6.332 | 1.461 | -22.52 | 1.46 |
| | | Set-2 | 7.2 | 1.249 | 2.4 | 6.805 | 1.270 | -25.82 | 1.46 |
| 124Sn | 23.3 | Set-1 | 15.0 | 1.305 | 2.5 | 7.739 | 0.984 | -52.55 | 1.37 |
| | | Set-2 | 15.0 | 1.252 | 2.8 | 7.446 | 0.961 | -47.26 | 1.27 |
| | 25.2 | Set-1 | 7.5 | 1.137 | 3.8 | 7.265 | 1.156 | -25.77 | 0.49 |
| | | Set-2 | 4.0 | 1.100 | 6.0 | 6.733 | 1.390 | -24.73 | 0.54 |
| | 27.7 | Set-1 | 0.3 | 1.161 | 4.5 | 7.590 | 0.978 | -12.06 | 3.39 |
| | | Set-2 | 0.1 | 1.161 | 7.5 | 6.990 | 1.125 | -18.92 | 3.79 |
| | 50.5 | Set-1 | 14.2 | 0.981 | 6.2 | 7.137 | 2.5242 | -56.70 | 4.00 |
| | | Set-2 | 5.0 | 0.644 | 8.2 | 7.415 | 2.4545 | -54.15 | 2.02 |

# Discussion and Conclusions

- Both the MSF and NM potentials satisfactorily describe the $\alpha$+$^{116,122,124}$Sn elastic scattering data.
- However, the MSF potential slightly overestimates the cross sections at 23.3, 25.2 and 27.7 MeV in the forward angles.
- The derived MSF potentials are free from renormalization for a satisfactory description of the data over the entire energy range.
- The radius of the unclustered nucleonic distribution is much less those of the $\alpha$-like clusters. This indicates that the alpha particle formation is energetically favoured in the surface region.

# Discussion and Conclusions

- In the case of NM potential, the fits are excellent using both unshifted repulsive core with $D_1 = 0$ and shifted repulsive core with $D_1 \neq 0$.
- The total $\chi^2$-value for potentials with $D_1 = 0$ and with $D_1 \neq 0$ are almost same.
- The potential with $D_1 = 0$ and that with $D_1 \neq 0$ mainly differ in the central region of the target nucleus.
- From the closeness of the fits to the data and the nearly same $\chi^2$-value suggest that the scattering is dominated by potentials at nuclear surface.

- Thus the MSF and NM potentials have been proved to be successful in explaining the $\alpha$ elastic scattering on $^{208}$Pb.
- More data with oscillatory refractive structure are required to completely study the nature of the $\alpha$ elastic scattering on Sn isotopes.

# THANK YOU FOR YOUR PATIENCE